

LENSING DISPERSION OF SNIa AND SMALL SCALES OF THE PRIMORDIAL POWER SPECTRUM

IDO BEN-DAYAN

Deutsches Elektronen-Synchrotron DESY, Theory Group, D-22603 Hamburg, Germany

Probing the primordial power spectrum at small scales is crucial for discerning inflationary models, especially if BICEP2 results are confirmed. We demonstrate this necessity by briefly reviewing single small field models that give a detectable gravitational waves signal, thus being degenerate with large field models on CMB scales. A distinct prediction of these small field models is an enhancement of the power spectrum at small scales, lifting up the degeneracy. We propose a way to detect this enhancement, and more generally, different features in the power spectrum at small scales $1 \lesssim k \lesssim 10^2 - 10^3 \text{ Mpc}^{-1}$ by considering the existing data of lensing dispersion in Type Ia supernovae. We show that for various deviations from the simplest $n_s \simeq 0.96$ the lensing dispersion cuts considerably into the allowed parameter space by PLANCK and constrains the spectrum to smaller scales beyond the reach of other current data sets.

1 Introduction

State of the art CMB and Ly_α measurements probe only about 8 e-folds, ($H_0 \lesssim k \lesssim 1 \text{ Mpc}^{-1}$) out of the expected 60 e-folds of observable inflation¹, rendering a huge degeneracy between inflationary models. Even a confirmation of the BICEP2 measurement², will not break all the degeneracy. For example, small field models with a non-monotonic ϵ reproduce a spectrum similar to that of a monomial $V \sim \phi^n$ for a limited range of wave numbers³. Even within the class of large field models there is a degeneracy that can only be lifted by probing enough e-folds of the power spectrum. The answer lies in probing smaller scales of the power spectrum. In⁴ we proposed using the lensing dispersion of type Ia supernovae as a novel cosmological probe and specifically as a constraint on the primordial power spectrum at small scales. See also⁵. The lensing dispersion, σ_μ is sensitive to $0.01 \lesssim k \lesssim 10^2 - 10^3 \text{ Mpc}^{-1}$, thus giving access to 2 – 3 more decades (4 – 7 e-folds) of the spectrum, even using only *current data*.

In the next section, we review the non-monotonic ϵ idea. In section 3 we present how the lensing dispersion probes the primordial power spectrum on small scales. Section 4 describes the results for various parameterizations of the spectra, complementing⁴, and some discussion.

2 Small field models and large r

Consider canonically normalized, single field models $V(\phi) = \Lambda^4 \sum_{n=0} a_n \phi^n$, assuming CMB scales are at $\phi \simeq 0$. Generically a_0 sets the scale of inflation, a_1 sets the tensor to scalar ratio $r = 16\epsilon$, a_2 sets n_s etc. A small field model $\Delta\phi < 1$ requires parametric tuning of a few parameters for a successful model of inflation, i.e. $\epsilon, |\eta| \ll 1$, to get 60 e-folds and $n_s \simeq 0.96$.^a This generically means $a_1 \ll 1$ and hence $r \ll 0.01$ in odds with the BICEP2 result^b. A large field generically means functional tuning, for

^aThe virtue of small field models, i.e. parametric tuning of only a few operators is especially relevant if one considers an inflation as a fundamental field. For effective low energy degrees of freedom, one can get $\Delta\phi \gg 1$ in a rather natural way⁶.

^bIn⁷, I erroneously claimed a non-monotonic ϵ evades the Lyth bound from 1996⁸, contributing to confusion in the literature. This was promptly corrected in³. The strict '96 bound cannot be evaded, only the BL bound⁹, which assumes a monotonic ϵ .

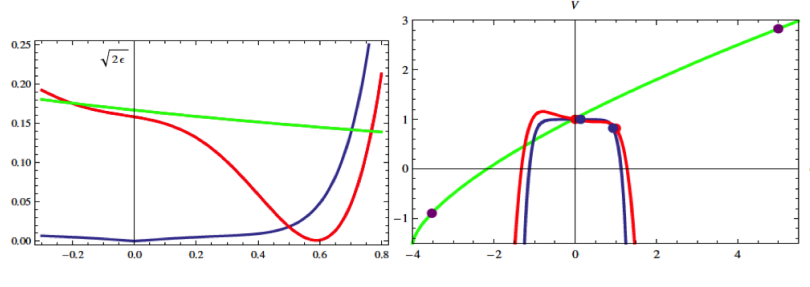


Figure 1 – $\sqrt{2\epsilon(\phi)}$ (left panel) and $V(\phi)$ (right panel) for typical hilltop (blue), monomial $V \sim \phi^{2/3}$ with a constant shift for clarity (green), and the non-monotonic ϵ models (red).

example $a_{n \neq 2} = 0$, for all n , which gives a free massive inflaton. Such models give $r \sim 0.1$, in accord with the BICEP2 findings. One would like a UV theory that explains the functional tuning we use. Moreover, taken at face value, the $r = 0.2$ BICEP2 result is in tension with PLANCK, unless the cosmological model is further extended to include primordial Helium, additional light degrees of freedom or a scale dependent spectral index $n_s(k)$, in a way that suppresses the power on intermediate scales. Regardless, hints of "running" $\alpha(k_0) \equiv dn_s/d \ln k$ have been around since WMAP1¹⁰.

Several years prior to PLANCK and BICEP2, in³ we demonstrated the key idea, that non-monotonic $\epsilon = \frac{1}{2} \left(\frac{V'}{V} \right)^2$ allows small field models to have $r \sim 0.1$, avoiding the need of functional tuning, which is especially interesting in light of BICEP2¹¹. If at CMB scales, ϵ is rather large, then from $r = 16\epsilon$ we get detectable signal, $r \sim 0.1$. However, away from the CMB scales, ϵ decreases, giving many e-folds of inflation, $N = \int d\phi / \sqrt{2\epsilon}$. In Figure 1, reproduced from³, we demonstrate the behaviour of $\sqrt{2\epsilon} = |V'/V|$ and the potential V as a function of the inflation. One can have an arbitrary number of e-folds in a very small interval $\Delta\phi \ll 1$ ^{3,12}. Therefore, the main limitation is the scale dependence of the power spectrum, $P \sim V/\epsilon$, since by now about 8 e-folds have been measured with limited amount of scale dependence parameterized by $\alpha(k_0) \equiv dn_s/d \ln k, \beta(k_0) \equiv d^2 n_s/d \ln k^2$.

Because of the non-monotonic ϵ , a distinct *prediction* of the models, which was made prior to PLANCK and BICEP2 results, is the enhancement of the power spectrum at small scales. In³ the spectrum was calculated numerically by solving the Mukhanov-Sasaki equation, and in¹³ it was argued that a spectrum with a bend at some k_i is a good approximation of the model, which we will use in section 4. Knowing the power spectrum at smaller scales is interesting by itself for a better understanding of inflation. Specifically, it can break the degeneracy between the above models and the monomial ones, because the former will have enhanced power at small scales^c. We therefore suggest the lensing dispersion of SNe as a probe of the small scale power spectrum and a novel cosmological probe in general.

3 Lensing Dispersion of SNIa

Using the light-cone averaging approach up to second order in the Poisson (longitudinal) gauge¹⁶, a simple expression for the lensing dispersion in⁴ was derived:

$$\sigma_\mu^2 \simeq \left(\frac{5}{\ln 10} \right)^2 \frac{\pi}{\Delta\eta^2} \int_{\eta_s^{(0)}}^{\eta_o} \frac{d\eta_1 dk}{k} P_\Psi(k, \eta_1) k^3 (\eta_1 - \eta_s^{(0)})^2 (\eta_o - \eta_1)^2, \quad (1)$$

$$\simeq \left(\frac{5}{\ln 10} \right)^2 \frac{\pi}{\Delta\tilde{\eta}^2} \left(\frac{k_{eq}}{H_0} \right)^3 \int d\tilde{\eta}_1 dp P_\Psi(p, \tilde{\eta}_1) p^2 (\tilde{\eta}_1 - \tilde{\eta}_s^{(0)})^2 (\tilde{\eta}_o - \tilde{\eta}_1)^2. \quad (2)$$

where η_o is the observer conformal time, $\eta_s^{(0)}$ is the conformal time of the source with unperturbed geometry, $\Delta\eta(z) = \eta_o(z) - \eta_s^{(0)}(z) = \int_0^z \frac{dy}{H_0 \sqrt{\Omega_{m0}(1+y)^3 + \Omega_{\Lambda 0}}}$, and P_Ψ is the linear (LPS, P_L) or non-linear dimensionless power spectrum (NLPS, P_{NL}) of the *gravitational potential*. In the second line we switched

^cMeasuring the spectrum for enough e-folds we will be able to discriminate even between the simplest models via spectral distortions¹⁴, and perhaps even get a hint of a stringy origin¹⁵.

to dimensionless variables, $\tilde{\eta} = H_0\eta$ and $p = k/k_{eq}$ ^d. Equation (2) demonstrates the relevant physical scales H_0 and k_{eq} , the sensitivity to scales smaller than the equality scale $p > 1$, and the expected enhancement pattern $(k_{eq}/H_0)^3$ in the linear regime and potentially additional $(k_{NL}/k_{eq})^3$ at a redshift dependent non-linearity scale, k_{NL} . So we have a direct probe of the integrated late-time power spectrum and of the cosmological parameters.

At redshift $z \sim 1$ the dispersion, σ_μ , grows approximately linearly with redshift, so the best constraints will be obtained from the maximal available redshift of current data, $z = 1$. We do not have a definite detection, but a conservative 2-sigma upper bound $\sigma_\mu(z = 1) \leq 0.12$ ¹⁷. It is conservative because all analyses^{16,17,18,19} point to a lower value of the dispersion, at most $\sigma_\mu(z) \simeq 0.093z$ ¹⁸. Moreover, the most up-to-date JLA analysis uses the actual value from¹⁷, $\sigma_\mu = 0.055z$ and still sees a decrease as a function of redshift in the left over 'coherent' or 'intrinsic' dispersion, suggesting that even the *total dispersion* at $z \simeq 1$ is only $\sigma_\mu^{tot} \lesssim 0.12$ ¹⁹. Additionally, partial sky coverage and higher redshift SN, which have already been used for cosmological parameter inference, will increase the dispersion, making our analysis even more conservative.

The main limitation of (2) is the validity of the spectrum¹⁶, because for $k \gg H_0$ standard cosmological perturbation theory breaks down, and one has to resort to numerical simulations to get an approximate fitting formula for the power spectrum. We use the HaloFit model²⁰ with $k_{UV} = 320h \text{ Mpc}^{-1}$. For the standard case $P_k = A_s(k/k_0)^{n_s(k_0)-1}$, $\sigma_\mu(z = 1, k_{UV} = 320h \text{ Mpc}^{-1}) \simeq 0.08$. Within a certain range, varying H_0, Ω_{m0}, k_{UV} can account at most for 15% difference⁴. Hence the bound cannot be saturated by varying the background parameters and/or integrating up to arbitrarily small scales. Hence, it can be used for probing small scales of the power spectrum. After fixing all the background parameters, including $A_s, n_s(k_0 = 0.05 \text{ Mpc}^{-1})$ to the most likelihood value of¹, we achieve accuracy of about 20%.

4 Results

We analyze four different, more general parameterizations of the spectrum and the corresponding panel in Figure 2:

$$P_k = A_s \left(\frac{k}{k_0} \right)^{n_s(k_0)-1 + \frac{\alpha(k_0)}{2} \ln \frac{k}{k_0} + \frac{\beta(k_0)}{6} \ln^2 \frac{k}{k_0}}, \quad \text{top left panel} \quad (3)$$

$$P_k = A_s \left(\frac{k}{k_0} \right)^{n_s(k_0)-1} + B \left(\frac{\pi e}{3} \right)^{3/2} \left(\frac{k}{k_i} \right)^3 e^{-\pi/2(k/k_i)^2}, \quad \text{top right panel} \quad (4)$$

$$P_k = A_s \left(\frac{k}{k_0} \right)^{n_s(k_0)-1} \left[1 + \frac{B}{A_s} \Theta(k - k_i) \right], \quad \text{bottom left panel} \quad (5)$$

$$P_k = A_s \left(\frac{k}{k_0} \right)^{n_s(k_0)-1} \left[\Theta(k_i - k) + \left(\frac{k}{k_i} \right)^{n_s^*(k_0)-1} \Theta(k - k_i) \right]. \quad \text{bottom right panel} \quad (6)$$

where Θ is the Heaviside function, $\alpha(k_0) \equiv dn_s/d \ln k$, $\beta(k_0) \equiv d^2 n_s/d \ln k^2$ are the "running" and "running of running" of the spectral index, (4) is a typical parameterization of one episode of particle production²¹, (5) describes a step in the power spectrum, for instance due to several episodes of inflation²², and (6) describes an enhancement which is not necessarily captured just by running. The models discussed in section 2 fit the latter parameterization.

For the above parameterizations, the HaloFit formula is not reliable anymore due to its sensitivity to initial conditions. It is nevertheless obvious that the non-linear evolution causes clustering and enhances the power spectrum. We therefore define a ratio, $F(k, z) \equiv \frac{P_{NL}(k, z)}{P_L(k, z)}$, where P_{NL} is the non-linear power spectrum, $P_L = (3/5)^2 P_k T^2(k) g^2(z)$ is the linear spectrum, $g(z)$ is the growth factor and $T(k)$ is the transfer function with baryons¹⁶, in the standard scenario $n_s \simeq 0.96$. We take the enhancement into

^dThe choice of the equality scale $p = k/k_{eq}$ is because we know the general behaviour of P_L , or more precisely, its transfer function $T(k)$ which is constant for $p < 1$ and scales like $p^{-2} \ln p$ for $p \gg 1$

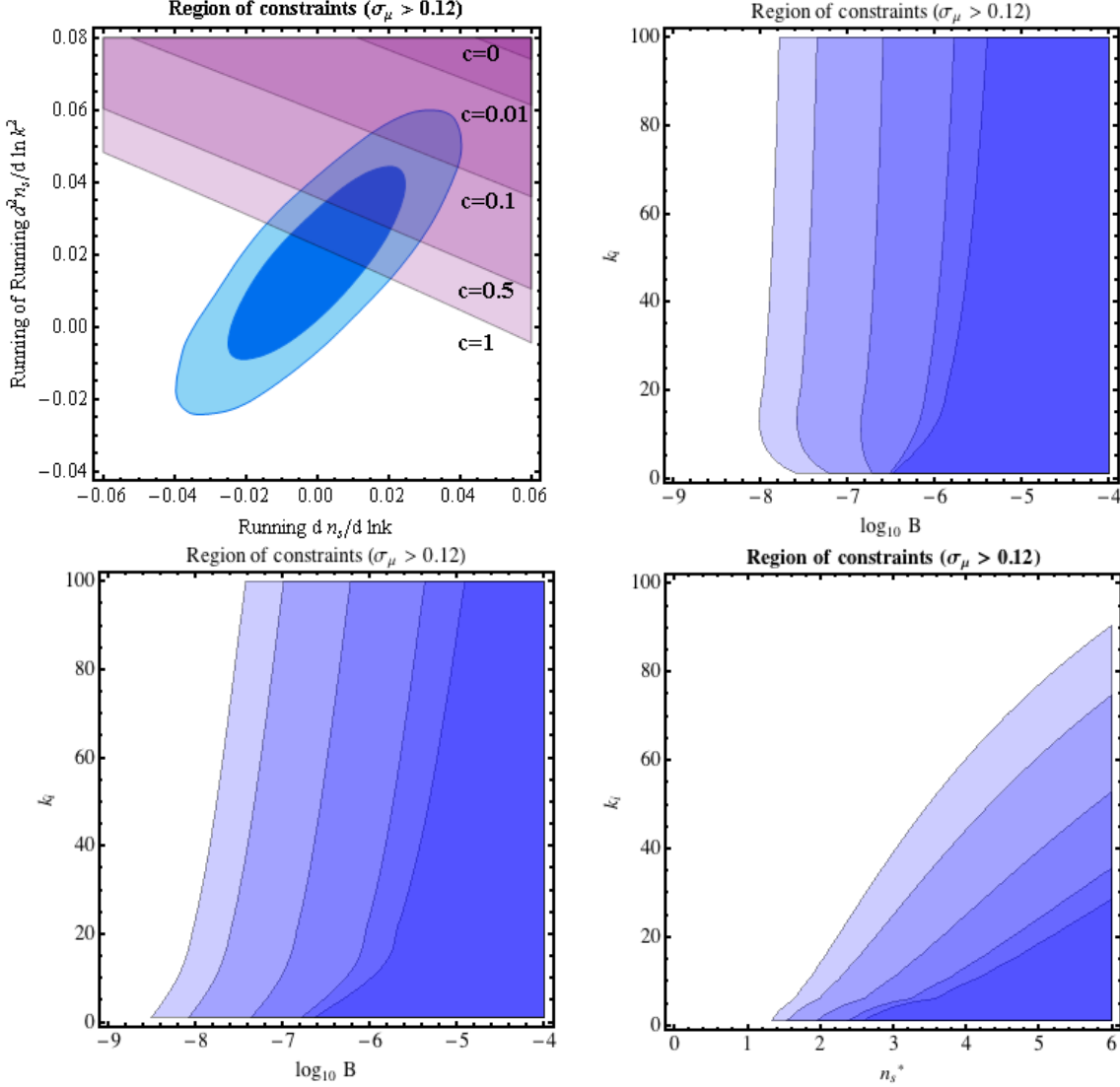


Figure 2 – Exclusion plots for the different parameterizations. Shaded regions correspond to $\sigma_\mu(z = 1) > 0.12$ with $c = 0, 0.01, 0.1, 0.5, 1$ respectively from dark to light and are disfavoured. The different parameterizations are: top left eq. (3), top right eq. (4), bottom left eq. (5), bottom right eq. (6). In the top left panel the ellipses correspond to 68% and 95% likelihood contours from PLANCK.

account by substituting in (1):

$$P_\Psi \rightarrow P_L(k, z)(1 - c + cF(k, z)), \quad (7)$$

and evaluate σ_μ with $c = 0, 0.01, 0.1, 0.5, 1$. $c = 0$ corresponds to computing the dispersion with the linear power spectrum only, while $c = 1$ corresponds to exactly following the HaloFit enhancement pattern. Except $c = 1$ all values of c are underestimates^e. The results are presented in Figure 2. In all panels, coloured regions give $\sigma_\mu(z = 1) \geq 0.12$ for $c = 0, 0.01, 0.1, 0.5, 1$ from dark to light and are disfavoured.

From Fig. 2, it is obvious that the lensing dispersion or its absence is an extremely powerful cosmological probe. Even if a scale dependent spectral index induces clustering which is *an order of magnitude smaller* than the standard constant n_s scenario, some of the parameter space allowed by PLANCK is ruled out. Moreover, the analysis probes the spectrum up to $k \sim 320h \text{ Mpc}^{-1}$, more than two orders of magnitude beyond PLANCK's lever arm (~ 5 e-folds more). Calling $c = 0.1$ 'realistic' and $c = 1$ 'optimistic',

^eIn⁴, we also considered a step function of the sort $P_\Psi \rightarrow P_L(k, z)(1 + b\Theta(k - k_{NL}))$, for $b = 0, 3, 10, 50$ with corresponding $k_{NL} = 1, 1, 2, 15 \text{ Mpc}^{-1}$ always underestimating the ratio F . The results are very similar to that of (7).

the spectrum never goes above $(6, 3.7) \times 10^{-7}$ up to $k \leq 320h \text{ Mpc}^{-1}$ respectively for features up to $k_i \leq 100 \text{ Mpc}^{-1}$. The only exception is (6) which gives $P_k(320h \text{ Mpc}^{-1}) = 2.3 \times 10^{-6}$ in the realistic case for $k_i \leq 50 \text{ Mpc}^{-1}$. This is due to a slow enhancement and on smaller scales so it is quickly erased via Silk damping. We are currently analyzing numerical simulations that will test our claims²³. Combining SN lensing in analyses (present and forthcoming missions), will undoubtedly allow a much better determination of the cosmological parameters.

Acknowledgments

We thank Tigran Kalaydzhyan for collaborating in the early stage of the work. This work is supported by the German Science Foundation (DFG) within the Collaborative Research Center (CRC) 676 “Particles, Strings, and the Early Universe”.

References

1. P. A. R. Ade *et al.* [Planck Collaboration], [arXiv:1303.5082 [astro-ph.CO]]. G. -B. Zhao *et al.*, Mon. Not. Roy. Astron. Soc. **436**, 2038 (2013) [arXiv:1211.3741 [astro-ph.CO]].
2. P. A. R. Ade *et al.* [BICEP2 Collaboration], Phys. Rev. Lett. **112**, 241101 (2014) [arXiv:1403.3985 [astro-ph.CO]].
3. I. Ben-Dayan and R. Brustein, JCAP **1009**, 007 (2010) [arXiv:0907.2384 [astro-ph.CO]].
4. I. Ben-Dayan and T. Kalaydzhyan, [arXiv:1309.4771 [astro-ph.CO]].
5. T. Hamana and T. Futamase, Astrophys. J. **534**, 29 (2000) [astro-ph/9912319]. E. M. Minty, A. F. Heavens and M. R. S. Hawkins, Mon. Not. Roy. Astron. Soc. **330**, 378 (2002) [astro-ph/0104221]. S. Dodelson and A. Vallinotto, Phys. Rev. D **74**, 063515 (2006) [astro-ph/0511086]. V. Marra, M. Quartin and L. Amendola, Phys. Rev. D **88**, 063004 (2013) [arXiv:1304.7689 [astro-ph.CO]]. M. Quartin, V. Marra and L. Amendola, Phys. Rev. D **89**, 023009 (2014) [arXiv:1307.1155 [astro-ph.CO]]. C. Fedeli and L. Moscardini, [arXiv:1401.0011 [astro-ph.CO]]. T. Castro and M. Quartin, MNRAS Letters 2014 443 (1): L6-L10 [arXiv:1403.0293 [astro-ph.CO]].
6. J. E. Kim, H. P. Nilles and M. Peloso, JCAP **0501**, 005 (2005) [hep-ph/0409138]. M. Berg, E. Pajer and S. Sjors, Phys. Rev. D **81**, 103535 (2010) [arXiv:0912.1341 [hep-th]]. I. Ben-Dayan, F. G. Pedro and A. Westphal, [arXiv:1404.7773 [hep-th]]. S. -H. H. Tye and S. S. C. Wong, [arXiv:1404.6988 [astro-ph.CO]]. I. Ben-Dayan, F. G. Pedro and A. Westphal, [arXiv:1407.2562 [hep-th]].
7. I. Ben-Dayan, [arXiv:0910.5515 [astro-ph.CO]].
8. D. H. Lyth, Phys. Rev. Lett. **78**, 1861 (1997) [hep-ph/9606387].
9. L. Boubekur and D. .H. Lyth, JCAP **0507**, 010 (2005) [hep-ph/0502047].
10. H. V. Peiris *et al.* [WMAP Collaboration], Astrophys. J. Suppl. **148**, 213 (2003) [astro-ph/0302225].
11. S. Choudhury and A. Mazumdar, arXiv:1403.5549 [hep-th]. F. Bezrukov and M. Shaposhnikov, arXiv:1403.6078 [hep-ph]. S. Antusch and D. Nolde, JCAP **1405**, 035 (2014) [arXiv:1404.1821 [hep-ph]]. Q. Gao, Y. Gong, T. Li and Y. Tian, Sci. China Phys. Mech. Astron. **57**, 1442 (2014) [arXiv:1404.7214 [hep-th]]. G. German, arXiv:1405.3246 [astro-ph.CO]. F. Brummer, V. Domcke and V. Sanz, arXiv:1405.4868 [hep-ph]. J. Bramante, S. Downes, L. Lehman and A. Martin, arXiv:1405.7563 [astro-ph.CO]. S. Antusch, F. Cefala, D. Nolde and S. Orani, arXiv:1406.1424 [hep-ph]. J. Rubio and M. Shaposhnikov, arXiv:1406.5182 [hep-ph].
12. N. Itzhaki and E. D. Kovetz, Class. Quant. Grav. **26**, 135007 (2009) [arXiv:0810.4299 [hep-th]].
13. J. Chluba, A. L. Erickcek and I. Ben-Dayan, Astrophys. J. **758**, 76 (2012) [arXiv:1203.2681 [astro-ph.CO]].
14. J. Chluba and D. Jeong, [arXiv:1306.5751 [astro-ph.CO]].

15. I. Ben-Dayan, S. Jing, A. Westphal and C. Wieck, JCAP **1403**, 054 (2014) [arXiv:1309.0529 [hep-th]].
16. M. Gasperini, G. Marozzi, F. Nugier and G. Veneziano, JCAP **1107**, 008 (2011) [arXiv:1104.1167 [astro-ph.CO]]. I. Ben-Dayan, M. Gasperini, G. Marozzi, F. Nugier and G. Veneziano, JCAP **1204**, 036 (2012) [arXiv:1202.1247 [astro-ph.CO]]. I. Ben-Dayan, M. Gasperini, G. Marozzi, F. Nugier and G. Veneziano, Phys. Rev. Lett. **110**, 021301 (2013) [arXiv:1207.1286 [astro-ph.CO]]. I. Ben-Dayan, G. Marozzi, F. Nugier and G. Veneziano, JCAP **1211**, 045 (2012) [arXiv:1209.4326 [astro-ph.CO]]. I. Ben-Dayan, M. Gasperini, G. Marozzi, F. Nugier and G. Veneziano, JCAP **1306**, 002 (2013) [arXiv:1302.0740 [astro-ph.CO]].
17. J. Jonsson *et al.*, [arXiv:1002.1374 [astro-ph.CO]].
18. D. E. Holz and E. V. Linder, Astrophys. J. **631**, 678 (2005) [astro-ph/0412173]. T. Kronborg *et al.* [SNLS Collaboration], [arXiv:1002.1249 [astro-ph.CO]]. N. V. Karpenka, M. C. March, F. Feroz and M. P. Hobson, [arXiv:1207.3708 [astro-ph.CO]]. M. Smith *et al.* [SDSS Collaboration], Astrophys. J. **780**, 24 (2014) [arXiv:1307.2566 [astro-ph.CO]].
19. M. Betoule *et al.* [SDSS Collaboration], [arXiv:1401.4064 [astro-ph.CO]].
20. K. T. Inoue and R. Takahashi, Mon. Not. Roy. Astron. Soc. **426**, 2978 (2012) [arXiv:1207.2139 [astro-ph.CO]].
21. N. Barnaby and Z. Huang, Phys. Rev. D **80**, 126018 (2009) [arXiv:0909.0751 [astro-ph.CO]].
22. J. A. Adams, G. G. Ross and S. Sarkar, Nucl. Phys. B **503**, 405 (1997) [hep-ph/9704286].
23. I. Ben-Dayan and R. Takahashi, (to appear).